Molecular Biology of the Cell
Vol. 17, 2896–2909, July 2006

Stat-mediated Signaling Induced by Type I and Type II Interferons (IFNs) Is Differentially Controlled through Lipid Microdomain Association and Clathrin-dependent Endocytosis of IFN Receptors

Marta Marchetti,*† Marie-Noelle Monier,*† Alexandre Fradagrada,* Keith Mitchell,* Florence Baychelier,‡ Pierre Eid,‡ Ludger Johannes,* and Christophe Lamaze*

*Laboratoire Trafic et Signalisation, UMR144 Curie/CNRS, Institut Curie, 75248 Paris Cedex 05, France; and ‡Laboratoire d'Oncologie Virale, CNRS-UPR 9045, 94801 Villejuif, France

Submitted January 26, 2006; Revised April 3, 2006; Accepted April 11, 2006
Monitoring Editor: Sandra Schmid

Type I (α/β) and type II (γ) interferons (IFNs) bind to distinct receptors, although they activate the same signal transducer and activator of transcription, Stat1, raising the question of how signal specificity is maintained. Here, we have characterized the sorting of IFN receptors (IFN-Rs) at the plasma membrane and the role it plays in IFN-dependent signaling and biological activities. We show that both IFN-α and IFN-γ receptors are internalized by a classical clathrin- and dynamin-dependent endocytic pathway. Although inhibition of clathrin-dependent endocytosis blocked the uptake of IFN-α and IFN-γ receptors, this inhibition only affected IFN-α–induced Stat1 and Stat2 signaling. Furthermore, the antiviral and antiproliferative activities induced by IFN-α but not IFN-γ were also affected. Finally, we show that, unlike IFN-α receptors, activated IFN-γ receptors rapidly become enriched in plasma membrane lipid microdomains. We conclude that IFN-R compartmentalization at the plasma membrane, through clathrin-dependent endocytosis and lipid-based microdomains, plays a critical role in the signaling and biological responses induced by IFNs and contributes to establishing specificity within the Jak/Stat signaling pathway.

INTRODUCTION

Interferons (IFNs) play key roles in mediating innate and acquired host immune responses against viral infections and exhibit antiproliferative and tumoricidal activity (Stark *et al.*, 1998; Schindler and Brutsaert, 1999). Type I IFN genes encode IFN-α (13 subtypes) and the structurally related IFN-β, IFN-κ, IFN-ω, and IFN-τ. IFN-γ is the only member of the type II family and is structurally different from type I IFNs. IFN-γ is encoded by a separate chromosomal locus but shares several cellular effects of type I IFNs (Schroder *et al.*, 2003). Both types of IFN transmit their signal through specific binding to distinct cell membrane receptors. These are the IFN-α/β receptor (IFNAR), composed of IFNAR1 and IFNAR2 subunits and the IFN-γ receptor (IFNGR), composed of IFNGR1 and IFNGR2 subunits (Bach *et al.*, 1997; Mogensen *et al.*, 1999). Although much is known about how cells respond to IFNs, there is little information on the molecular characteristics of IFNAR and IFNGR endocytosis and thus, on the role of IFN receptor (IFN-R) endocytosis in IFN physiology.

Receptor endocytosis has classically been viewed as a passive means for terminating signaling through lysosomal degradation of activated receptor complexes after being internalized from the cell surface. However, Vieira *et al.* (1996) demonstrated an active role for endocytosis through clathrin-coated pits in EGF-R signaling, and it has become increasingly apparent that for several transducing receptors endocytosis and signaling may be tightly coordinated (Ceresa and Schmid, 2000; Di Fiore and De Camilli, 2001; Sorkin and Von Zastrow, 2002). Endocytosis through clathrin-coated pits and vesicles has long been considered the main endocytic process for transmembrane receptors in mammalian cells (Brodsky *et al.*, 2001). However, recent studies have definitely established that alternative endocytic routes exist, grouped under the generic term of clathrin-independent endocytosis (Conner and Schmid, 2003). The molecular details of these pathways are still poorly understood, and their physiological roles in cells have yet to be established (Johannes and Lamaze, 2002). Lately, clathrin-independent endocytosis has been considered to occur through cholesterol- and sphingolipid-enriched membrane domains, that is, lipid rafts and caveolae (Parton, 2003). Initially, lipid rafts have been defined biochemically as detergent-resistant membrane microdomains (DRMs) that are enriched in glycosphingolipids and cholesterol (Brown and London, 2000). Therefore, the finding that IFNAR and IFNGR were associated with membrane microdomains (Takaoka *et al.*,

This article was published online ahead of print in *MBC in Press* (http://www.molbiolcell.org/cgi/doi/10.1091/mbc.E06–01–0076) on April 19, 2006.

† These authors contributed equally to this work.

Address correspondence to: Christophe Lamaze (christophe.lamaze@curie.fr).

Abbreviations used: DRM, detergent resistant membrane; IFN-R, interferon receptor; IFNAR, interferon alpha receptor; IFNGR, interferon gamma receptor; RNAi, RNA interference; Stat, signal transducer and activator of transcription; Tf, transferrin.

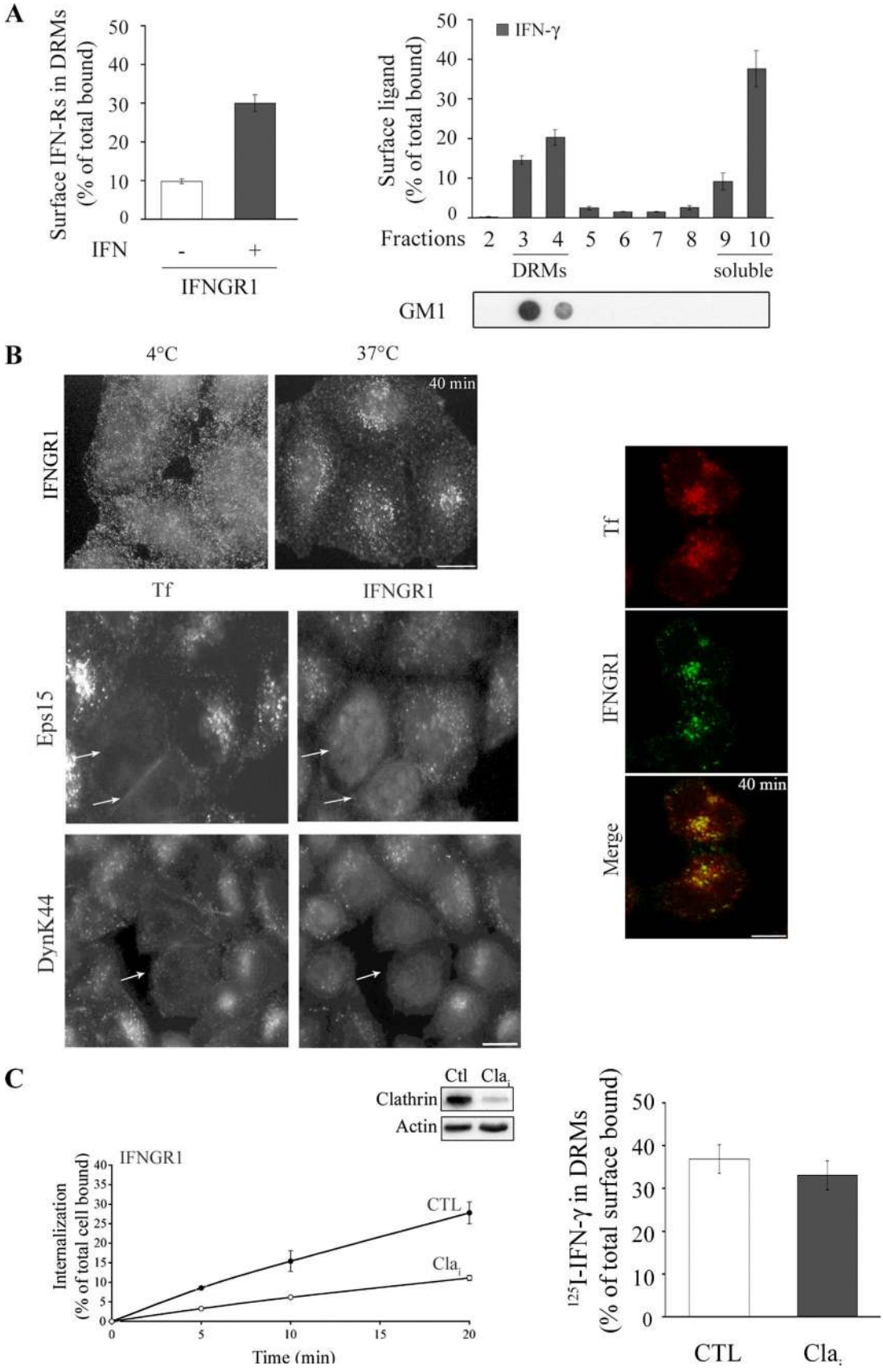

Figure 1. Plasma membrane compartmentalization and endocytosis of IFNGR1 complexes. (A) IFN-γ stimulates IFNGR complexes association with plasma membrane DRMs. Left, HeLaM cells were incubated at 4°C with ^{125}I-GIR94, a nonneutralizing mAb against IFNGR1,

2000) has suggested that IFN-R uptake may occur through a raft-mediated process (Subramaniam and Johnson, 2002) as described for the clathrin-independent internalization of the interleukin-2 receptor (Lamaze *et al.*, 2001).

Here, we have investigated the respective roles of membrane microdomain association and clathrin-dependent endocytosis in the trafficking and signaling of the IFN-Rs. We show that the efficient uptake of IFNAR and IFNGR complexes occurs through classical clathrin- and dynamin-dependent endocytosis. We also show that receptor binding with IFN-γ only results in the rapid association of activated IFNGR complexes with lipid microdomains of the plasma membrane. Finally, we demonstrate that IFN-R endocytosis is required for activating the transcription factor Stat1 and for the biological responses induced by IFN-α but not IFN-γ. Thus, the activation of Stat1, a downstream effector common to both IFN-α and IFN-γ, is selectively controlled through lipid microdomain association and clathrin-dependent endocytosis of the IFN-Rs. Altogether, our results show that membrane compartmentalization and endocytosis of the IFN-Rs play a critical, and previously unsuspected, role in the specificity of IFN-induced signaling and biological activity.

MATERIALS AND METHODS

Cell Culture and Transfection

HeLaM cells were maintained in Dulbecco's modified Eagle's essential medium (DMEM) supplemented with 10% fetal bovine serum (FBS), and L929R1R2 cells, murine fibroblasts stably expressing IFNAR1 and IFNAR2, were cultured as described (Cajean-Feroldi *et al.*, 2004). Dynamin-HeLa cells conditionally expressing the K44A mutated form of dynamin-1 were cultured in DMEM with 10% fetal calf serum, 1% L-glutamine, 400 μg/ml geneticin, 200 ng/ml puromycin, and 1% penicillin/streptomycin. Dynamin-HeLa cells were routinely grown in the presence of 1 μg/ml tetracycline. For expression of the dominant negative K44A mutant, cells were grown in the absence of tetracycline for 48 h (Damke *et al.*, 1994). For transient transfections, cells were grown on glass coverslips, transfected using FuGene (Roche, Meylan, France) or the Calcium Phosphate kit (Invitrogen, Carlsbad, CA), and processed 24 h later for fluorescent microscopy analysis.

Figure 1 (cont). before treatment with (■) or without (□) IFN-γ for 3 min at 37°C. DRMs were prepared, and the percentage of surface IFNGR1 subunits present in DRMs was measured by the amount of radioactivity counted in pooled DRM fractions. GM1 was detected by dot-blot with Cholera toxin–HRP. Right, HeLaM cells were incubated with ^{125}I-IFN-γ for 3 min at 37°C, and sucrose gradient fractionation was performed. The amount of ^{125}I-IFN-γ present in each fraction was expressed as the percentage over total cell surface bound iodinated IFN-γ. Results are representative of at least three independent experiments. (B) Top, the cell surface distribution of IFNGR1 subunits was visualized at 4°C by immunostaining of HeLaM cells. Endocytosis of IFNGR1 was detected by visualizing internalized antibody/IFNGR1 subunits complexes after an acid wash. Right, confocal microscopy analysis of the colocalization of internalized Cy5-Tf and IFNGR1-antibody–bound complexes. Bottom, HeLaM cells were transfected with a plasmid encoding the GFP-Eps15 mutant or with a plasmid encoding the GFP-dyn2 (ba) K44A mutant. In transfected cells (arrows), both Tf and IFNGR1 uptake were inhibited. Scale bars 10 μm. (C) Left, IFNGR1 endocytosis was quantitatively measured in CHC RNAi-treated HeLaM cells using avidin inaccessibility. Inset shows the level of clathrin heavy-chain expression detected by immunoblotting of lysates from RNAi-treated (Cla_i) and nontreated (Ctl) HeLaM cells. Right, HeLaM cells transfected (■) or not (□) with the CHC RNAi plasmid were incubated for 3 min at 37°C with ^{125}I-IFN-γ, and DRMs were prepared. Radioactivity was counted and the amount of ^{125}I-IFN-γ present in DRMs was expressed as the percentage of total cell surface bound ^{125}I-IFN-γ. Results are representative of at least three independent experiments.

RNA Interference

RNA interference (RNAi)-treated cells were transfected with the pSuper vector containing the human CHC RNAi oligonucleotide as previously described (Saint-Pol *et al.*, 2004). Cells were used 4 d after transfection.

IFNs, Antibodies, and Plasmids

Recombinant human IFN-α2b (specific activity of 10^8 U/mg) from Biosidus (Buenos Aires, Argentina) was provided by J. Wietzerbin and IFN-γ (specific activity of 2×10^7 U/mg) was from RDI (Flanders, NJ). Mouse anti-IFNAR1 monoclonal antibody (mAb) 64G12 and mAb 34F10 were as previously described (Cajean-Feroldi *et al.*, 2004), and mouse anti-IFNGR1 mAb GIR94 was from Transduction Laboratories (Lexington, KY). Mouse anti-IFNAR1 mAb AA3, a gift from Biogen (Boston, MA), and mouse anti-IFNAR2 mAb (RDI); rabbit anti-Tyk2, and anti-Jak1 pAb (Cell Signalling, Beverly, MA); and rabbit anti-Stat1 pAb and mouse mAb RC20-HRPO (Transduction Laboratories) were used in immunoprecipitation experiments. Other antibodies were as follows: rabbit anti-phospho-Stat1 (Tyr701) and anti-Stat1 pAb from Cell Signalling Technology, rabbit anti-phospho-Stat2 (Tyr689) and anti-Stat2 pAb from Upstate Biotechnology, mouse anti-clathrin mAb heavy chain (Transduction Laboratories), and mouse anti-actin mAb AC-74 (Sigma, St. Louis, MO). Tf-Cy5, Tf-Cy3, and the plasmid encoding the EH domain of GFP-Eps15 were as previously described (Lamaze *et al.*, 2001). The plasmid encoding the GFP-dyn2 (ba) K44A mutant of dynamin 2 was provided by M. McNiven.

Immunofluorescence and Endocytosis Assays

Endocytosis analysis by immunofluorescence was carried out as previously described (Lamaze *et al.*, 2001). Briefly, cells grown on coverslips were incubated on ice with the corresponding anti-IFN-R subunit mAb and/or Tf-Cy5 for 40 min. The cells were washed and incubated at 37°C in the presence of 1000 U/ml IFN-α or IFN-γ for the indicated time. The antibody-receptor complexes remaining at the cell surface were eliminated by incubating the cells in ice-cold ascorbate buffer at pH 4.5 for 30 min. Cells were washed, fixed, and permeabilized. Antibody/IFN-R subunits that had undergone endocytosis were revealed with a rabbit Cy3-conjugated anti-mouse pAb (Jackson ImmunoResearch, West Grove, PA). Coverslips were mounted and the cells were imaged with an epifluorescent Leica microscope or a confocal Leica SP2 microscope (Deerfield, IL; Figure 1B, right panel). The rate and extent of IFNAR1 and IFNGR1 endocytosis were measured by avidin inaccessibility as previously described (Vieira *et al.*, 1996). For IFNGR1, a biotinylated-GIR94 mAb was used (PharMingen, San Diego, CA). For IFNAR1, 64G12 mAb was biotinylated using 3.8 μg of NHS-SS-Biotin (Pierce, Rockford, IL). Serum-starved cells were detached from plates with 2 mM phosphate-buffered saline (PBS)/EDTA, and 1.5×10^5 cells were incubated with 5 μg/ml biotin-GIR94 or biotin-64G12 for 30 min on ice. After washing, cells were incubated at 37°C in the presence of 1000 U/ml IFN-α or IFN-γ for the indicated times, and endocytosis was stopped by cooling to 4°C. Surface-bound biotin-mAbs were quenched with an excess of avidin, which was then neutralized with biocytin. Cells lysates were loaded on ELISA plates coated with rabbit anti-mouse IgG pAb. Free biotin-GIR94 and biotin-64G12 antibodies corresponding, respectively, to IFNGR1 and IFNAR1 subunits that had undergone endocytosis were detected with streptavidin-HRP (Roche).

Radiolabeling and Scatchard Analysis

IFN-α2b (Imgenex, San Diego, CA) and IFN-γ (RDI) were radiolabeled with iodine-125 using the chloramine T method as previously described (Lamaze *et al.*, 2001). Nonneutralizing mAb 34F10 and mAb GIR94 were iodinated using the iodobead method following the manufacturer's instructions (Pierce). The apparent equilibrium dissociation constant, K_d, and the number of binding sites per cell were measured by Scatchard analysis. Cells were detached with 2 mM PBS/EDTA, counted, and incubated for 2 h at 4°C with increasing concentrations of ^{125}I-IFN-α2b, from 0.25 to 8 nM, and increasing concentrations of ^{125}I-IFN-γ, from 0.15 to 5 nM. Parallel ^{125}I-IFN-α and ^{125}I-IFN-γ binding assays were carried out in the presence of a 200-fold excess of unlabeled IFN-α and IFN-γ to determine nonspecific binding. Cells were washed three times, and pellets and washes were counted using a gamma counter to quantify the respective amounts of bound and free ligand.

Preparation of Detergent-resistant Membranes

The amount of IFNAR1 and IFNGR1 subunits present in DRMs of the plasma membrane was quantified by first incubating cells with iodinated antibodies for 1 h at 4°C. These were then washed and incubated or not with 1000 U/ml IFN-α2b or IFN-γ for 3 min at 37°C. Alternatively, cells were incubated for 3 min at 37°C with ^{125}I-IFN-α or ^{125}I-IFN-γ. DRMs were prepared by fractionation of Triton X-100 cell lysates on a discontinuous sucrose density gradient as previously described (Lamaze *et al.*, 2001). After ultracentrifugation, the radioactivity present in each fraction was counted using a gamma counter.

Surface IFNGR1 subunits associated with DRMs were immunoprecipitated by incubating cells at 4°C with mAb GIR94. These were then washed and stimulated or not with IFN-γ for 3 min at 37°C. DRMs were prepared and each gradient fraction was solubilized by incubation with 1% Triton X-100 and 2% BSA for 15 min at 37°C. All DRM fractions (3–4), and two-fifths of the

soluble fractions (9–10) were pooled separately and incubated with protein G-Sepharose (Amersham, Arlington Heights, IL) for 2 h at 4°C. The immunoprecipitates were resolved by SDS-PAGE and analyzed for phospho-tyrosine residues and IFNGR1 subunits by Western blotting. When indicated, cells were treated for 30 min at 37°C with filipin (5 μg/ml; Sigma) before stimulation with IFN-γ and maintained during the incubation with mAb GIR94 at 4°C.

IFN-induced Stimulation of Stat

Cells were grown in 0.5% FBS medium for 24 h and then in serum-free medium for 30 min before the experiment. Cells were treated with or without 1000 U/ml IFN-α2b or IFN-γ at 37°C for the indicated times. For biochemical analysis, cells were washed with PBS at 4°C and lysed in SDS sample buffer. Total lysates were resolved on SDS-PAGE and analyzed by Western blot/ECL. For immunofluorescent analysis of Stat1 nuclear translocation, cells grown on coverslips were treated with IFN and fixed with cold methanol at −20°C for 10 min. After washing with cold PBS, cells were incubated with primary anti-phospho-Stat1 antibody overnight at 4°C, and antibody binding was revealed by incubation with a FITC-conjugated goat anti-rabbit secondary antibody (Jackson ImmunoResearch).

Nuclear and Cytoplasmic Fractions Preparation

Cytoplasmic and nuclear extracts were prepared from cells treated with or without IFN-α2b or IFN-γ for the indicated times. Cells were washed with ice-cold PBS and lysed in 0.5% Triton X-100/PBS on ice containing soybean trypsin inhibitor (5 μg/ml), leupeptin (5 μg/ml), and benzamidin (1.75 μg/ml). Cells were centrifuged at 3000 rpm for 10 min, and the supernatant (C) and the pellet (N) fractions were collected. Equal amounts of protein from each fraction were used for SDS-PAGE and Western blot/ECL analysis.

Plasma Membrane Isolation

Plasma membranes were isolated using a cationic colloidal silica-based technique adapted from Stolz *et al.* (1999). Dynamin K44A expression was induced or not in cells, which were then treated or not with IFN-α2b or IFN-γ by incubation for 3 min at 37°C. Cells, 20×10^6, were mechanically lysed, mixed with Nycodenz (50% final,) and overlaid on 0.5 ml of 70% Nycodenz in a SW55 centrifuge tube (25 min at 20,000 × *g*). The silica content in the pellet and the 50–70% interface were collected and washed, and equal amounts were immunoblotted for phospho-Stat1 and Stat1. Lysates and isolated plasma membranes were assayed for total protein content (Bradford), the plasma membrane marker alkaline phosphodiesterase (APDE), the lysosomal marker β-hexosaminidase (beta-hex), and the Golgi marker mannosidase (Manno). Results were expressed as the increase in enrichment of the different markers present in the isolated plasma membrane fractions versus total cell lysate.

Immunoprecipitations

Dynamin K44A mutant expression was induced or not in 3×10^6 dynamin HeLa cells, which were then lysed in RIPA buffer. Cell lysates were centrifuged at 3000 rpm for 10 min, and the supernatant was incubated overnight at 4°C with the indicated antibody. Protein A-Agarose beads were added at a 1:10 ratio (vol/vol) and incubated for 2 h at 4°C. After washing, the beads were resuspended in SDS sample buffer, and the immunoprecipitate proteins were resolved on SDS-PAGE and analyzed by Western blot/ECL. Immunoblots were quantified from appropriate exposures using the NIH Image software.

Luciferase Reporter Assay

HeLaM cells were transfected with the ISG54-luciferase construct (0.5 μg), provided by S. Pellegrini, or the pGAS-TA-luciferase construct (0.5 μg), provided by Y. Gaudin, and cotransfected with the empty pcDNA vector (mock) or dynamin K44A (1 μg) using Lipofectamine 2000 (Invitrogen). After 48 h, cells were treated with 1000 U/ml recombinant IFN-α2b, or IFN-γ for 8 h. Luciferase activity was quantified in cell lysates using a luminometer (Lumat LB9501, Berthold, Wildbad, Germany), and results were expressed as the percentage of total activity measured in control (mock-transfected) cells.

Antiviral Assay

The antiviral assay was carried out as previously described using a cytopathic effect reduction assay with a vesicular stomatitis virus (vsv) at a multiplicity of infectivity = 0.1–1.6 (Rubinstein *et al.,* 1981). Control and CHC RNAi-treated cells (2×10^4, Cla_i) or 1.8×10^4 dynamin HeLa cells, in which K44A mutant expression was or was not induced, were grown on a microtiter dish overnight. Cells were treated for 24 h with 1:2 serial dilutions of a 2000 U/ml starting concentration of IFN-α2b, or IFN-γ, as indicated, and the virus was added for 24 h. Cells were stained with crystal violet, and the absorption at 595 nM was measured. The results are given as a function of serial dilutions of IFN.

Table 1. Scatchard analysis of HeLaM and HeLa dynamin cells

	IFN-α		IFN-γ	
	K_d (nM)	No. of sites/cell	K_d (nM)	No. of sites/cell
HeLaM	2.47	7,630	0.79	26,550
HeLaM Cla_i	2.64	11,010	1.13	54,920
HeLa dyn	2.35	1,990	0.08	7,110
HeLa dynK44A	2.80	2,520	0.14	10,140

HeLaM cells were transfected (Cla_i) or not with the clathrin heavy-chain RNAi plasmid, and HeLa dynamin cells were induced or not for dyn K44A expression. Binding assays of ^{125}I-IFN-α and ^{125}I-IFN-γ were done in duplicate as described in *Material and Methods.*

Antiproliferative Assay

The antiproliferative activities of IFN-α and IFN-γ were analyzed in control and CHC RNAi-treated HeLaM cells according to the MTT assay as previously described (Vieira *et al.,* 1996).

RESULTS

The Role of Lipid Microdomains and Clathrin in the Uptake of IFNGR Complexes

Few studies have investigated the distribution of IFN-Rs at the plasma membrane. Previous studies showed that some gold-labeled IFN-α and IFN-γ could be found in clathrin-coated pits in B lymphocytes (Zoon *et al.,* 1983; Filgueira *et al.,* 1989), whereas more recent studies have shown that IFNAR and IFNGR complexes were associated with raft-type membrane microdomains in lymphocytes and epithelial WISH cells (Takaoka *et al.,* 2000; Subramaniam and Johnson, 2002). We aimed to evaluate the relative contribution that each of these two processes plays in the uptake of activated IFN-Rs. We first analyzed the distribution of IFN-Rs at the plasma membrane in HeLaM cells, an HeLa cell line that responds fully to IFN-α and IFN-γ stimulation (Tiwari *et al.,* 1987). Scatchard analysis showed that HeLaM cells expressed large amounts of IFNGR and IFNAR complexes (Table 1). Cells were incubated at 4°C with nonneutralizing iodinated antibodies against the extracellular domain of IFNGR1, lysed with Triton X-100, and then centrifuged through discontinuous sucrose gradients. This biochemical assay allowed to collect DRMs, which were found in fractions that were positive for the lipid raft marker glycosphingolipid GM1 (Figure 1A). At steady state, ~10% of the total pool of IFNGR1 subunits present at the plasma membrane were found in DRM fractions (Figure 1A). On receptor activation, we detected a significant association of IFNGR1 with DRMs (30% of the total surface pool) as early as 3 min after addition of IFN-γ at 37°C (Figure 1A). Nonspecific effects due to antibody cross-linking were ruled out by directly examining the association of surface receptor-bound IFN with DRMs by incubating cells with iodinated IFN-γ for 3 min at 37°C. Again, we detected almost 40% of the total surface bound ^{125}I-IFN-γ in DRMs (Figure 1A). We found similar results in Jurkat lymphocytes and in epithelial WISH cells, ruling out cell type specificities (unpublished data).

A number of multichain immune receptors have been found associated with DRMs, although the significance of this remains unclear (Dykstra *et al.,* 2001). Because IFNGR complexes associate with caveloae-like microdomains, it has been proposed that IFNGR complexes selectively under-

went endocytosis through raft-type lipid microdomains (Subramaniam and Johnson, 2002). Therefore, we aimed to characterize the endocytic pathways followed by endogenous IFNGR complexes in HeLaM cells in the presence of IFN-γ. We observed by immunofluorescence that at 4°C IFNGR1 subunits were uniformly distributed in fine punctate pattern on the cell surface (Figure 1B). We also observed a similar distribution for IFNGR2 subunits (unpublished data). Uptake of IFNGR1 subunits occurred after the temperature was increased to 37°C, with subunits being seen in many endocytic structures. After 40 min, we found IFNGR1 in a perinuclear endosomal compartment together with cointernalized transferrin (Tf; Figure 1B).

We next tested the effect of molecular inhibitors that selectively block clathrin-dependent uptake. We first investigated Eps15, a protein selectively required for the assembly of clathrin-coated pits (Benmerah *et al.*, 1998). As a control, Tf endocytosis was blocked in cells transfected with a dominant negative GFP-tagged mutant of Eps15 (Figure 1B, arrows). We found that IFNGR1 uptake was completely inhibited in these cells. We also blocked clathrin-dependent endocytosis by expressing a dominant negative mutant of the GTPase dynamin. This GTPase is required for detaching clathrin-coated pits from the plasma membrane (Damke *et al.*, 1994). In cells expressing the K44A dynamin mutant, Tf endocytosis was inhibited together with IFNGR1 uptake (Figure 1B, arrows). These data strongly suggested that endocytosis of IFNGR complexes was mediated through clathrin-coated pits. We then used a recently developed RNA interference (RNAi) tool to down-modulate clathrin heavy-chain (CHC) expression (Saint-Pol *et al.*, 2004) to evaluate further the contribution of the clathrin machinery in IFNGR uptake. Immunoblotting showed that CHC RNAi treatment of the cells led to 80% inhibition of CHC expression (Figure 1C). Using a quantitative endocytosis assay, we measured <10% of the normal IFNGR1 uptake after allowing endocytosis to proceed for 20 min in CHC RNAi-treated cells, a residual rate typical for nonspecific uptake through bulk-flow endocytosis. Altogether, these results clearly demonstrate that IFNGR complexes use the classical clathrin- and dynamin-dependent endocytic pathway for their efficient uptake into cells. We also found that the absence of functional clathrin-coated pits at the plasma membrane had no effect on the extent of IFN-γ association with DRMs (Figure 1C), implying that the association of activated IFNGR complexes with DRMs and their endocytosis through clathrin-coated pits were separate events.

The Role of Lipid Microdomains and Clathrin in the Uptake of IFNAR Complexes

Because HeLaM cells also expressed large amounts of IFNAR complexes, we were able to analyze and compare the behavior of IFNAR complexes within the same cell system. Cells were incubated at 4°C with a nonneutralizing iodinated antibody against the extracellular domain of IFNAR1, and DRMs were collected as described above. Under basal conditions, we found that the amount of IFNAR1 subunits in DRMs was the same as that for IFNGR1 subunits; that is, 10% of the total pool of cell-surface complexes. However, unlike for IFNGR1, receptor binding by IFN-α did not increase the association of IFNAR1 with DRMs (Figure 2A). Likewise, incubation of the cells with iodinated IFN-α for 3 min at 37°C did not change the basal level of association with DRMs. We never observed any increase in the association of IFNAR complexes with DRMs after ligand binding or anti-IFNAR1 antibody cross-linking in any of the different conditions and cell types used (unpublished data). We next investigated the role of clathrin-dependent endocytosis in the uptake of activated IFNAR complexes. Using the quantitative assay described above, we found that CHC RNAi treatment strongly inhibited IFNAR1 endocytosis, with a residual uptake level being close to background levels (Figure 2B). Consistent with the inhibition of clathrin-dependent uptake, Scatchard analysis showed a twofold increase in the number of IFNGR and IFNAR complexes present at the cell surface of CHC RNAi-treated cells. Likewise, IFNAR and IFNGR complexes were equally retained at the cell surface of K44A dynamin-expressing cells (Table 1). The mAb against IFNAR did not work for the immunofluorescent detection of internalized IFNAR complexes in HeLaM and HeLa dynamin cells. However, using mouse fibroblasts that express larger amounts of human IFNAR1 and IFNAR2 subunits (Cajean-Feroldi *et al.*, 2004), we observed clathrin-, dynamin-, and Eps15-dependent IFNAR1 uptake by immunofluorescence (Figure 2C). After allowing endocytosis to proceed for 40 min at 37°C, we also found IFNAR1 in a perinuclear endosomal compartment together with cointernalized Tf (unpublished data). These results show that after cell activation by IFNs, there are major differences between IFNAR and IFNGR complexes in their association with lipid microdomains of the plasma membrane. However, both complexes share the classical clathrin- and dynamin-dependent endocytic pathway for their efficient uptake into cells.

Stat Activation Is Impaired in IFNAR Endocytosis-deficient Cells

Previous work has suggested that IFNGR endocytosis and IFN-γ dependent signaling were independent events (Farrar *et al.*, 1991; Kerr *et al.*, 2003). IFN-mediated signaling predominantly relies on tyrosine kinases of the Janus kinase family that preassociate with IFN-Rs: Jak1 and Tyk2 for IFNAR, and Jak1 and Jak2 for IFNGR. The activation of these kinases by IFN-α or IFN-γ leads to the phosphorylation of IFNAR1 or IFNGR1 subunits, respectively, thereby creating docking sites for the cytoplasmic transcription factor Stat1. On receptor recruitment, Stat1 is phosphorylated on Tyr-701 by Jak1 or Jak2 (Taniguchi and Takaoka, 2001). IFN-α also leads to the recruitment of Stat2 to IFNAR1 and to phosphorylation on Tyr-690, which is required for the binding of Stat1 to Stat2 (Stark *et al.*, 1998). Although the central role played by Stat molecules in IFN-induced signaling is well understood, the molecular mechanisms regulating the formation and transport of activated Stat-signaling complexes from the plasma membrane to the nucleus remain obscure (Levy and Darnell, 2002). Therefore, we aimed to determine whether lipid-based compartmentalization of IFN-Rs at the plasma membrane and/or clathrin-dependent endocytosis contributes to Stat-mediated IFN signaling.

In HeLaM cells, we detected Stat1 and Stat2 activation, that is tyrosine phosphorylation, as early as 3 min after IFN-α stimulation, which continued for up to 30 min (Figure 3A). We observed a similar behavior for Stat1 activation after IFN-γ stimulation. By contrast, in cells in where IFNAR endocytosis was blocked by CHC RNAi treatment, Stat1 and Stat2 tyrosine phosphorylation was strongly reduced after 3 min of stimulation with IFN-α, remained affected for 20 min, and returned to control values after 30 min of IFN-α treatment (Figure 3A). Unexpectedly, we found that Stat1 activation induced by IFN-γ was normal in CHC RNAi-treated cells (Figure 3A), even as early as 1 min after IFN-γ stimulation (unpublished data). This ruled out different IFN-α– and IFN-γ–induced Stat1 kinetics as causing a lack of effect. Similar effects were observed in CHC RNAi-treated WISH cells (unpublished data). We also studied Stat-dependent

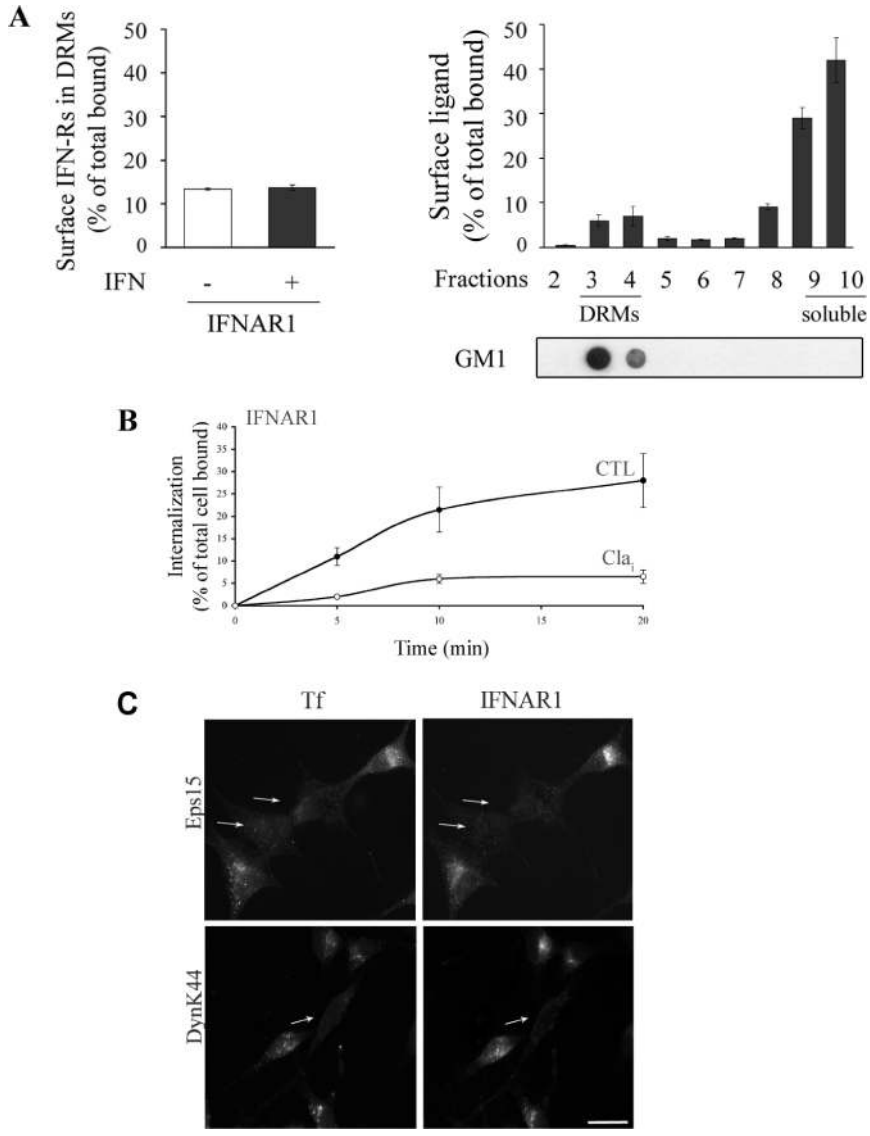

Figure 2. Plasma membrane compartmentalization and endocytosis of IFNAR1 complexes. (A) Left, IFN-α does not stimulate the association of IFNAR complexes with plasma membrane DRMs. HeLaM cells were incubated at 4°C with ^{125}I-34F10, a nonneutralizing mAb against IFNAR1, before treatment with (■) or without (□) IFN-α for 3 min at 37°C. DRMs were prepared, and the percentage of surface IFNAR1 subunits present in DRMs was measured by the amount of radioactivity counted in pooled DRM fractions. GM1 was detected by dot-blot with Cholera toxin-HRP. Right, HeLaM cells were incubated with ^{125}I-IFN-α for 3 min at 37°C, and sucrose gradient fractionation was performed. The amount of ^{125}I-IFN-α present in each fraction was expressed as a percentage of total cell surface bound iodinated IFN-α. Results are representative of at least three independent experiments. (B) IFNAR1 endocytosis was quantitatively measured in CHC RNAi-treated HeLaM cells using avidin inaccessibility. (C) Eps15 and dynamin are required for endocytosis of IFNAR1. L929R1R2 cells were transfected with a plasmid encoding the GFP-Eps15 mutant or the GFP-dyn2 (ba) K44A mutant. In transfected cells (arrows), both Tf uptake and the endocytosis of IFNAR1 were inhibited. Scale bars, 10 μm.

signaling in HeLa dynamin cells as expression of the dynamin K44A mutant immobilizes the clathrin-coated pits that are fully assembled at the plasma membrane (Damke *et al.*, 1994). After IFN-α and IFN-γ stimulation, Stat1 and Stat2 tyrosine phosphorylation kinetics in control HeLa dynamin cells were similar to those observed in HeLaM cells. In K44A dynamin-expressing cells, IFN-α–induced Stat1 and Stat2 tyrosine phosphorylation was reduced to the same extent as for CHC RNAi-treated cells. Again, we observed no difference between control and K44A dynamin-expressing cells after IFN-γ stimulation (Figure 3A). Altogether, these results provide the first molecular evidence that endocytosis through clathrin-coated pits is required to ensure the correct activation of Stat1 and Stat2 by IFN-α. Although IFNGR complexes are also internalized by clathrin-dependent endocytosis, the activation of Stat1 by IFN-γ is independent from IFNGR endocytosis.

Blocking IFNAR Endocytosis Affects Stat1 Activation at the Plasma Membrane

We next looked for the molecular defects responsible for inhibiting Stat1 activation by IFN-α in cells in which clathrin-dependent endocytosis had been blocked. Although Scatchard analysis showed that the number of IFN-Rs present at the cell surface increased after dynamin K44A expression or CHC RNAi treatment, the affinity of IFNAR and IFNGR complexes for their respective ligands was not changed (Table 1). On average, HeLaM cells expressed four times more IFNAR and IFNGR complexes at the cell surface than dynamin HeLa cells, showing that differences in the number of receptors did not influence the effect of endocytosis inhibition on IFN signaling. We also studied the pool of activated and nonactivated Stat1 present at the plasma membrane. Coating the cells with cationic silica increases the density of the plasma membrane allowing it to be isolated by gradient centrifugation (Stolz *et al.*, 1999). The plasma membranes obtained under these conditions represented ~10% of the total cellular proteins and were, on average, enriched sevenfold in the selective plasma membrane marker APDE (Figure 3B). IFN stimulation and/or expression of the dynamin K44A mutant did not effect the purity and yield of isolated plasma membranes. We found that Stat1 was already present in the isolated plasma membranes before IFN-α or IFN-γ treatment. This was consistent

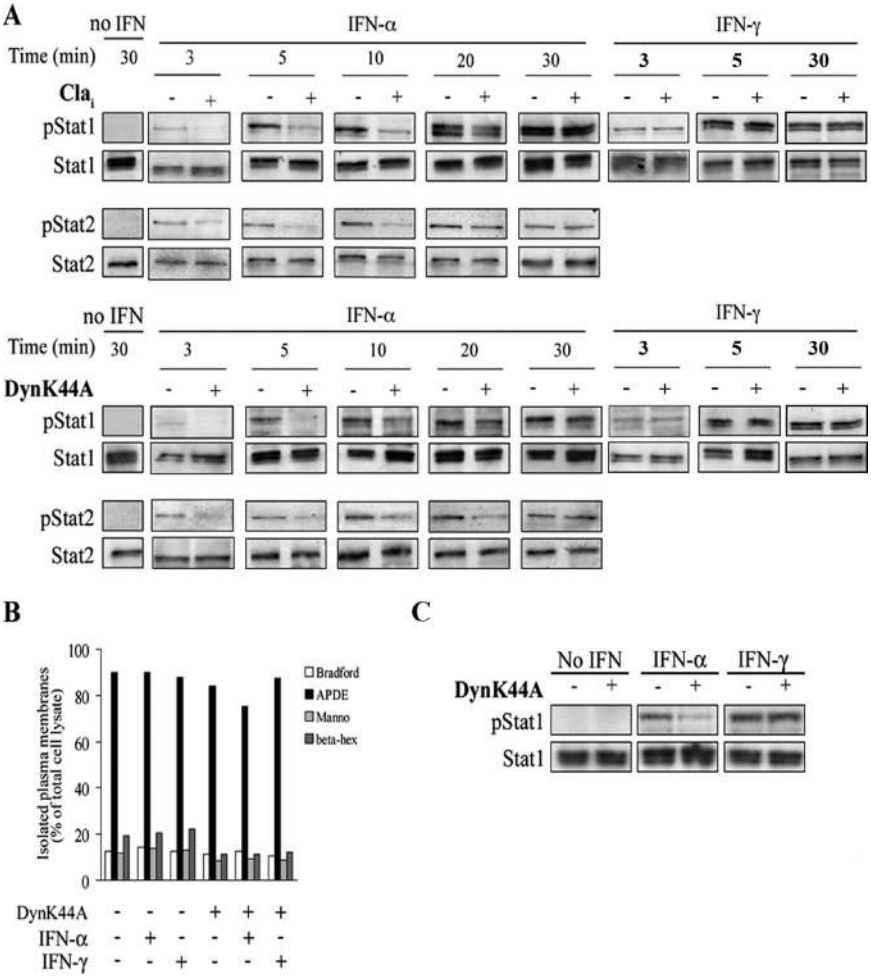

Figure 3. IFNAR but not IFNGR endocytosis is required for stat activation. (A) Top, HeLaM cells were transfected (+) or not (−) by the CHC RNAi plasmid (Cla_i) as indicated. Bottom, dynamin HeLa cells were induced (+) or not (−) for the expression of the K44A mutant as indicated. Cells were treated with 1000 U/ml IFN-α2b or IFN-γ at 37°C for the indicated times. Untreated cells are shown for control. Total lysates were analyzed by Western blot/ECL to detect phosphorylated Stat1 (pStat1) and Stat2 (pStat2) as indicated. Results are representative of at least three independent experiments. (B) Dynamin HeLa cells expressing (+) or not (−) K44A dynamin were treated for 3 min at 37°C with or without 1000 U/ml IFN-α2b or IFN-γ as indicated, and plasma membranes were isolated by silica coating. Left, the enrichment of the isolated membranes in different selective enzymatic markers of several cellular compartments including alkaline phosphodiesterase (APDE), β-hexosaminidase (beta-hex), and mannosidase (Manno). Right, equal protein amounts were analyzed in isolated plasma membranes by Western blot/ECL for phospho-Stat1 and Stat1 as indicated. Results are representative of at least three independent experiments.

with studies showing that Stat2, and possibly Stat1, can associate with the nonactivated, nonphosphorylated IFNAR complexes before ligand binding (Li *et al.*, 1997; O'Shea *et al.*, 2002). Stimulation of the cells with IFN-α or IFN-γ did not noticeably change the amount of Stat1 present on isolated plasma membranes (Figure 3B). However, we observed a marked decrease in the amount of tyrosine-phosphorylated Stat1 in plasma membranes isolated from K44A dynamin-expressing cells stimulated by IFN-α. The amount of activated Stat1 present in plasma membranes of K44A dynamin-expressing cells was normal after IFN-γ treatment (Figure 3B), consistent with IFN-γ–induced Stat1 activation being independent of IFNGR endocytosis (Figure 3A). Therefore, these results show that the inhibition of IFNAR endocytosis primarily results in a defect of Stat tyrosine phosphorylation at the plasma membrane rather than a defect in the amount of Stat1 recruited to IFNAR complexes.

Stat1 and Stat2 activation relies on the activation, by tyrosine phosphorylation, of the Jak1 and Tyk2 tyrosine kinases, which preassociate with IFNAR2 and IFNAR1 subunits, respectively (O'Shea *et al.*, 2002). In K44A dynamin-expressing cells, tyrosine phosphorylation of Tyk2 and Jak1 was strongly reduced early in the activation with respect to control cells (Figure 4, A and B). The tyrosine phosphorylation kinetics of Tyk2 and Jak1 in K44A dynamin-expressing cells corresponded to the tyrosine phosphorylation kinetics observed for Stat1 and Stat2, suggesting that the reduced activation of Stat1 and Stat2 in receptor endocytosis-deficient cells was due to the reduced activity of Tyk2 and Jak1 kinases. The similar association of Tyk2 with IFNAR1 and Jak1 with IFNAR2 in both control and receptor endocytosis-deficient cells (Figure 4C) ruled out a defect in the association of the kinases with IFNAR complexes blocked in nonfunctional clathrin-coated pits.

Blocking IFNAR Endocytosis Prevents Stat1 Nuclear Translocation

We investigated whether IFNAR uptake inhibition would also affect the nuclear translocation of activated Stat1, the endpoint of signaling within the Jak/Stat pathway (Kisseleva *et al.*, 2002). First, we used immunofluorescence to visualize the nuclear translocation of activated Stat1. In cells in which receptor uptake was blocked, as shown by inhibited Tf uptake, IFN-α did not induce nuclear translocation of Stat1 (Figure 5A, arrows). Although clathrin-dependent endocytosis also mediated the uptake of IFNGR (Figure 1, B and C), the nuclear translocation of Stat1 induced by IFN-γ was independent from the internalization process. We also studied the pattern of Stat1 tyrosine phosphorylation in nuclear and cytoplasmic fractions isolated by cell fractionation. In cells in which IFNAR uptake was inhibited by CHC RNAi treatment, we found a marked decrease in the amount of activated Stat1 in the cytoplasmic fractions after 5 and 10 min of stimulation with IFN-α (Figure 5B, top panel). Likewise, we detected almost no activated

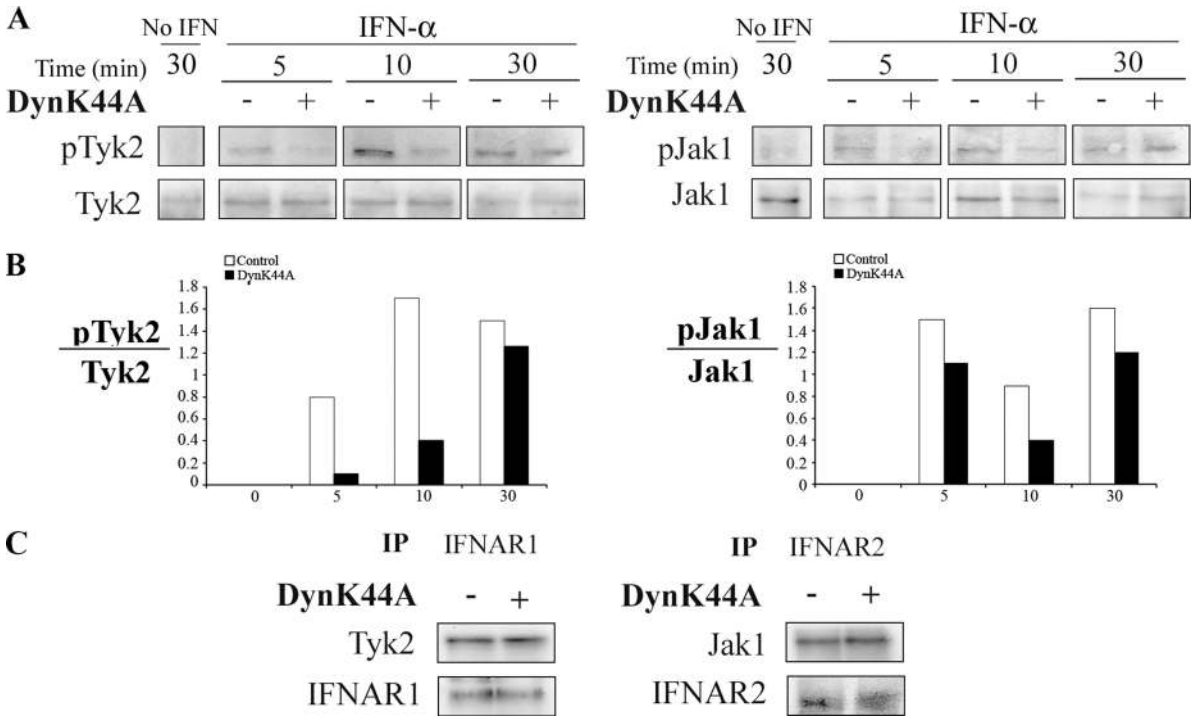

Figure 4. IFNAR endocytosis controls the activation of Jak1 and Tyk2. (A) Dynamin HeLa cells expressing (+) or not (−) the K44A mutant were treated for 3 min at 37°C with or without 1000 U/ml IFN-α2b as indicated. Cell lysates were analyzed by Western blot/ECL for Tyk2 and phosphorylated Tyk2 (pTyk2) and for Jak1 and phosphorylated Jak1 (pJak1). Untreated cells are shown for control. (B) Immunoblot images in A were quantified using the NIH Image software, and the ratio of the pTyk2 to Tyk2 and pJak1 to Jak1 signals were plotted to normalize the degree of tyrosine phosphorylation to the total levels of Tyk2 and Jak1 kinases. (C) IFNAR1 and IFNAR2 were immunoprecipitated from dynamin HeLa cells expressing (+) or not (−) the K44A mutant and analyzed by Western blot for their association with Tyk2 and Jak1 kinases, respectively. Blots were stripped and immunoblotted for IFNAR1 and IFNAR2.

Stat1 in the corresponding nuclear fractions. Consistent with previous results, the amount of activated Stat1 in the cytoplasmic and nuclear fractions of IFN-γ–treated cells was identical in both control and CHC RNAi-treated cells. Similar results were obtained in dynamin K44A-expressing cells (Figure 5B, bottom panel).

IFN-γ Early Signaling Correlates with the Association of IFNGR Complexes with DRMs

Several recent reports have shown that lipid-based compartmentalization may play a key role in the initial steps of signal transduction by immune receptors (Dykstra *et al.*, 2003). Therefore, we wanted to determine whether the increased association of IFNGR complexes with DRMs upon IFN-γ treatment was coupled to IFN-γ–mediated signaling. As shown above, IFN-γ binding increased the amount of cell surface IFNGR1 subunits in DRM fractions (Figure 5C). We analyzed whether DRM-associated IFNGR was part of an active signaling complex by probing cell surface IFNGR1 immunoprecipitates for tyrosine phosphorylation, which is an initial signaling event that couples activated IFNGR complexes with Stat1 activation (Schroder *et al.*, 2003). Indeed, after IFN-γ treatment, we found that most of the tyrosine phosphorylated IFNGR1 subunits were present in DRM fractions (Figure 5C). Filipin, which destabilizes the integrity of lipid microdomains through membrane cholesterol sequestration (Simons and Ikonen, 1997), prevents IFNGR1 subunits from associating with DRMs, with most being recovered in the soluble fractions from the gradient centrifugation. Under this condition, we observed almost no tyrosine phosphorylated IFNGR1 subunits present in the soluble fractions. Altogether, these results indicate that initiation pathways of IFNGR signaling may be assembled and activated in specialized plasma membrane microdomains, independent from IFNGR uptake through clathrin-coated pits.

Gene Transcription and Biological Responses Induced by IFN-α But Not IFN-γ Are Impaired in Cells Defective for IFN-R Endocytosis

Finally, we investigated whether the early reduction of Stat1 and Stat2 activation observed in receptor endocytosis-deficient cells could alter later signaling events such as gene transcription induction and the onset of biological responses. The transcription of IFN-α–stimulated genes (ISGs) depends on the binding of ISGF3 to IFN-stimulated response element (ISRE). ISGF3 is a multimeric transcription factor composed of phosphorylated Stat1 and Stat2 associated with p48 (IRF-9). We analyzed the transcription of ISRE element–containing genes by cotransfection of HeLaM cells with the dynamin K44A mutant and an ISRE-luciferase reporter construct. The transcriptional activity of HeLaM cells transfected with dynamin K44A was reduced by 50% 8 h after stimulation with saturating concentrations of IFN-α (Figure 6A). Gene transcription induced by IFN-γ stimulation occurs preferentially through the formation of phosphorylated Stat1 homodimers that bind to the GAS elements of target genes. Using a GAS luciferase reporter construct, we found that, unlike for IFN-α, the inhibition of receptor endocytosis in K44A dynamin-expressing cells did not affect IFN-γ–inducible gene transcription (Figure 6A). It is known that

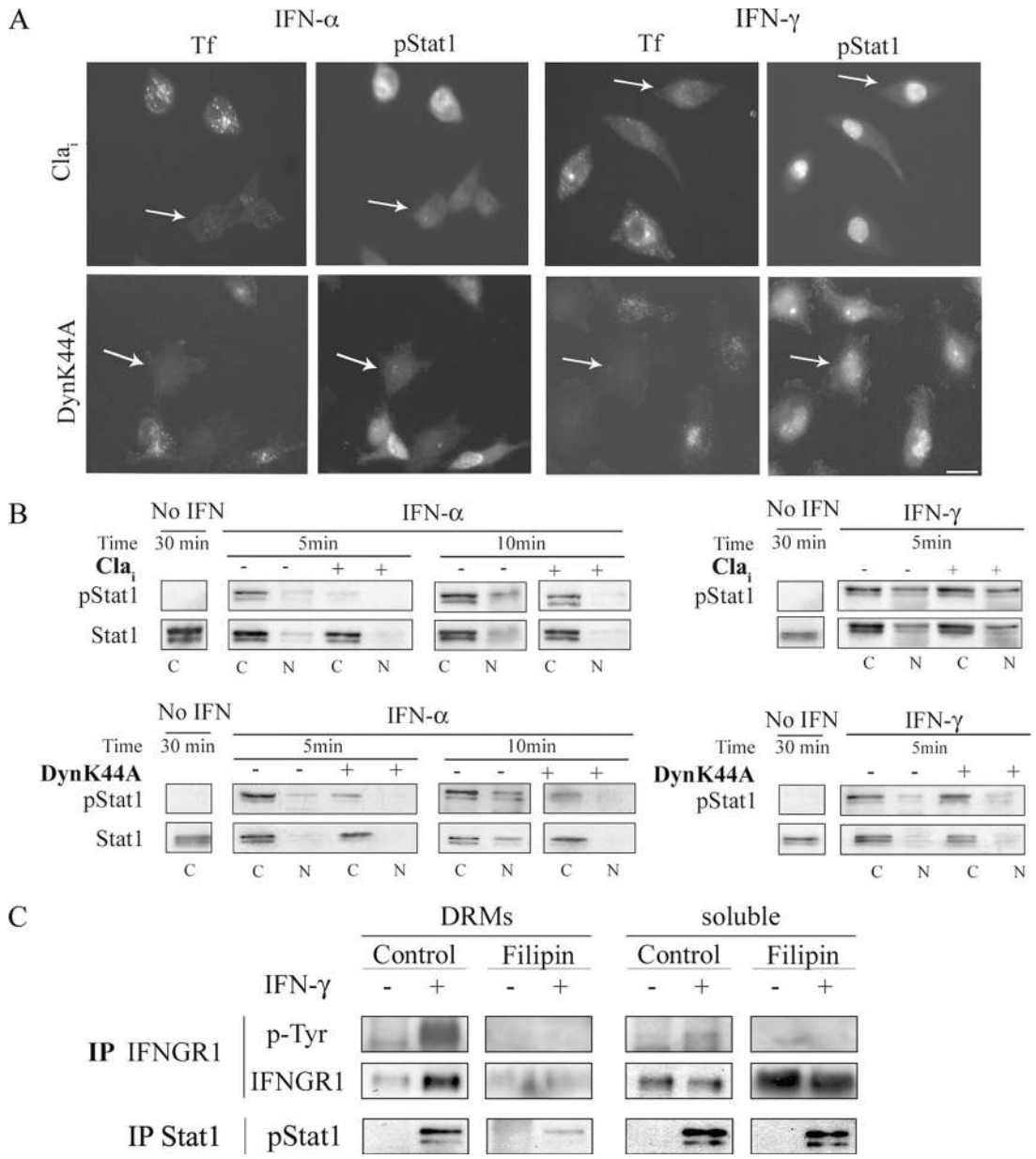

Figure 5. IFN-R endocytosis is required for IFN-α but not IFN-γ late signaling. (A) Analysis of the nuclear translocation of Stat1. HeLaM cells were treated with the CHC RNAi plasmid (Cla_i) or transfected with a plasmid encoding the GFP-tagged dynamin K44A mutant as indicated. Cells were treated for 5 min with 1000 U/ml IFN-α2b or IFN-γ and fixed, and the nuclear distribution of phospho-Stat1 was detected by immunofluorescence. Cy3-Tf was cointernalized for 5 min at 37°C to indicate cells inhibited for receptor endocytosis (arrows). Scale bar, 10 μm. Results are representative of at least three independent experiments. (B) Top, HeLaM cells were transfected (+) or not (−) by the CHC RNAi plasmid (Cla_i) as indicated. Bottom, dynamin HeLa cells were induced (+) or not (−) for the expression of the K44A mutant as indicated. Cells were treated with 1000 U/ml IFN-α2b or IFN-γ at 37°C for 5 and 10 min. After centrifugation, supernatant (C for cytoplasmic) and pellet (N for nuclear) fractions were collected, and equal amounts were immunoblotted for phospho-Stat1 and Stat1, as indicated. Untreated cells are shown for control. (C) Using mAb GIR94, IFNGR1 complexes were immunoprecipitated from the surface of HeLaM cells after treatment or not with IFN-γ and incubated or not with filipin, as indicated. Immunoprecipitates were recovered from DRMs and soluble fractions and resolved on SDS-PAGE analysis as described in *Materials and Methods.* IFNGR1 immunoprecipitates were immunoblotted for activated IFNGR1 (p-Tyr) and IFNGR1 subunits. Stat1 was immunoprecipitated from soluble and DRM fractions and immunoblotted for tyrosine phosphorylated Stat1 (pStat1).

IFN-γ is also able to activate the transcription of ISRE element–containing genes, although to a lesser extent. Again, the level of gene transcription activity was normal in K44A dynamin-transfected cells.

We then investigated whether the dysregulation of Stat-dependent signaling caused by the inhibition of IFNAR uptake would also affect the characteristics of the biological responses induced by IFN-α. First, we monitored the induction of IFN-dependent antiviral activity using a classical cytopathic assay. In control HeLaM and HeLa dynamin cells, IFN-α or IFN-γ were highly efficient at protecting against cell death induced by a vesicular stomatitis virus infection, with 50% protection at treatments as low as 2 U/ml IFN-α and 25 U/ml IFN-γ (Figure 6B). By contrast,

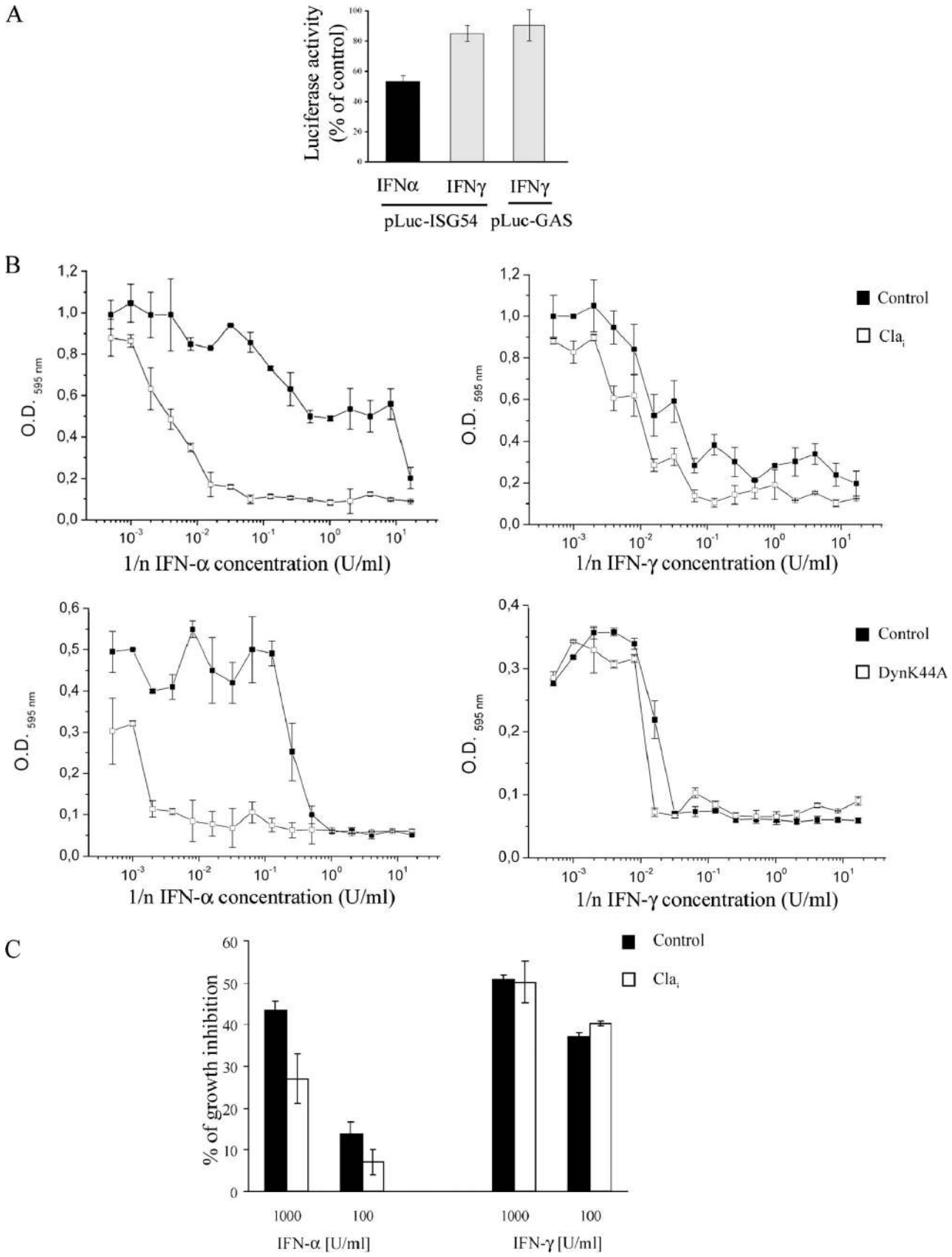

Figure 6. Gene transcription and biological responses induced by IFN-α but not IFN-γ are impaired in cells defective for IFN-R endocytosis. (A) HeLaM cells were cotransfected with the ISG54-luciferase or the pGAS-luciferase reporter constructs and the dynamin K44A plasmid.

IFN-α–induced antiviral activity was strongly reduced in cells in which IFN-R endocytosis was inhibited by either CHC RNAi treatment or dynamin K44A expression. We were unable to achieve a full antiviral response in cells expressing the dynamin K44A mutant even at IFN-α doses of up to 2000 U/ml. Although IFN-R endocytosis-defective cells did not respond to IFN-α, their antiviral activity remained intact after treatment with IFN-γ. We observed similar effects in WISH cells transfected with K44A dynamin (unpublished data). We then explored the impact of IFN-R endocytosis on controlling cell growth. As expected, IFN-α and IFN-γ showed strong antiproliferative effects, with treatments of 1000 and 100 U/ml IFN-α, respectively, reducing the growth rate of HeLaM cells by 45 and 15% (Figure 6C). CHC RNAi treatment reduced the IFN-α–induced antiproliferative activity by 50%. Under the same conditions, IFN-γ–inducible growth inhibition was not affected.

DISCUSSION

It is important to understand how specificity is maintained among the different signaling pathways propagated by multiple cytokine receptor complexes through limited and common downstream effectors (Levy and Darnell, 2002; Shuai and Liu, 2003). This is particularly relevant for type I and type II IFNs as they represent a family of 18 closely related molecules that bind to only two receptor complexes, IFNAR and IFNGR, transmitting their signal through the Jak/Stat cascade. Although it is now known that receptor endocytosis can control the activation and propagation of signaling responses (Ceresa and Schmid, 2000; Di Fiore and De Camilli, 2001; Wiley and Burke, 2001; Sorkin and Von Zastrow, 2002; Le Roy and Wrana, 2005), the molecular regulation of IFN-R endocytosis, and thus its role in IFN signaling, have not been investigated. We used different and selective approaches to inhibit receptor endocytosis, to show that IFNAR and IFNGR complexes are both internalized by a classical clathrin- and dynamin-dependent endocytic pathway. Based on studies with IFNGR, it had been assumed that IFN-R signaling and trafficking were independent events (Farrar *et al.*, 1992; Kerr *et al.*, 2003). However, we showed that clathrin-dependent endocytosis of activated IFNAR complexes is required for Stat-dependent signaling and for the biological responses induced by IFN-α.

Although further studies of the precise mechanisms by which clathrin-dependent endocytosis regulates IFN-α–induced Stat signaling are needed, we suggest several possibilities. Pioneering studies on the EGF-R have led to the concept of "signaling endosomes" from which signal transduction continues after being initiated at the plasma membrane (Vieira *et al.*, 1996; Miaczynska *et al.*, 2004). This model suggests that IFNAR endocytosis would regulate the delivery of activated receptors and associated molecules, such as Stat1 and Stat2, to endosomes to propagate signal transduction. This model was recently proposed for the activation of Stat3 by EGF as activated Stat3 was found in clathrin-derived vesicles present in the perinuclear region, and the inhibition of EGF-R endocytosis blocked Stat3-dependent nuclear translocation and gene transcription but not Stat3 tyrosine phosphorylation (Bild *et al.*, 2002). It is therefore unlikely that this model describes IFN-α–dependent Stat activation because Stat1 and Stat2 tyrosine phosphorylation was strongly reduced in endocytosis-deficient cells, and activated Stat1 and IFNAR complexes were not found in endocytic vesicles (unpublished data). Alternatively, clathrin-coated pits may be required for organizing distinct signaling platforms at the plasma membrane. This has been suggested for G protein–coupled receptors in which trafficking and signaling are coordinated by β-arrestins, scaffolding adaptor proteins that bind to clathrin and activated receptors (Shenoy and Lefkowitz, 2003). Although the Stat1 and Stat2 activation defect observed in CHC RNAi-treated cells having no clathrin-coated pits favors such a model, it is inconsistent with the decreased activation in K44A dynamin-expressing cells of Tyk2 and Jak1 kinases, showing that signaling was still affected despite the presence of fully assembly clathrin-coated pits at the plasma membrane. The early defect in Stat activation we observed in plasma membranes isolated from dynamin-inactivated cells suggests that clathrin-coated pits may regulate over time the association and dissociation of factors regulating the level of activation of IFNAR complexes and associated signaling molecules recruited to clathrin-coated pits. Although these factors currently remain unidentified, a recent study has shown that Jak/Stat signaling, which is required for cell border migration in *Drosophila* ovaries, was blocked in *Shibire* mutants, the fly homologue of dynamin (Silver *et al.*, 2005). The overexpression of the cytokine signaling suppressors SOCS 36E also blocked Jak/Stat-dependent cell migration to the same extent in *Drosophila.* SOCS is a family of negative feedback regulators of the Jak/Stat pathway that block Jak or Stat function (Fujimoto and Naka, 2003). Whether SOCS activity is coordinated with the endocytosis of activated IFN-R needs to be established. Further investigations, such as ultrastructural studies on the localization at the plasma membrane of Tyk2, Jak1, and other molecules of the IFNAR signaling complex, and mutational analysis of the receptor subunits are needed to determine more precisely the mechanisms of IFN-α signaling control by receptor trafficking.

We found that although activated IFNGR complexes were also internalized through clathrin-coated pits, IFN-γ–induced Stat1 signaling was not controlled by receptor endocytosis. By focusing on the plasma membrane, we found a major difference between the compartmentalization of activated IFNAR and IFNGR complexes. Although IFNAR and IFNGR complexes did not associate with plasma membrane DRMs at steady state, ligand binding to IFNGR but not IFNAR resulted in the rapid association of a significant amount of activated IFNGR complexes with DRMs. Whether DRM association truly reflects a protein being present in a lipid microdomain is still being debated (Munro, 2003). However, recent live cells experiments combined with theoretical modeling suggest that raft-type lipid microdomains

Figure 6 (cont). After 48 h, cells were treated with 1000U/ml recombinant IFN-α2b or IFN-γ for 8 h. Luciferase activity was quantified in cell lysates and expressed as the percentage of total activity measured in mock plasmid-transfected cells. The experiments were performed at least three times. (B) The antiviral response was analyzed by using a cytopathic effect reduction assay in cells infected with vsv. Top, HeLaM cells were transfected (□) or not (■) with the CHC RNAi plasmid (Cla_i). Bottom, dynamin HeLa cells were induced (□) or not (■) for dynamin K44A mutant expression. Cells were treated for 24 h with 1:2 serial dilutions of a 2000 U/ml starting concentration of IFN-α2b or IFN-γ as indicated, and vsv was added for 24 h. Cells were stained with crystal violet, and absorbance at 595 nM was measured. Results are the means of three independent experiments and are represented as a function of serial dilutions of IFN. (C) HeLaM cells transfected (□) or not (■) by the CHC RNAi plasmid (Cla_i) were starved for 24 h and incubated with 1000 or 100 U/ml IFN-α2b or IFN-γ for 72 h. Results are the means of two independent experiments and are expressed as the percentage of growth inhibition in cells treated with IFN in comparison to nontreated cells.

are highly dynamic nanometer-sized membrane domains that can assemble into larger structures (Sharma *et al.*, 2004). Indeed, several studies have suggested that signaling events at the plasma membrane may be mediated through functional lipid-based clustering resulting in signaling molecules engaging with cognate effectors in signaling platforms (Dykstra *et al.*, 2001; Harder and Engelhardt, 2004). The disruption of lipid-dependent clustering by cholesterol sequestration markedly reduced the tyrosine phosphorylation of the IFNGR1 subunit, an early event upstream of Stat1 phosphorylation, strongly suggesting that the integrity of these specialized lipid-based microdomains is essential for assembling and initiating IFN-γ–induced early signaling at the plasma membrane. Remarkably, the inhibition of clathrin-dependent endocytosis did not stop activated plasma membrane IFNGR complexes from associating with DRMs, further demonstrating that lipid microdomain-dependent IFN-γ early signaling and IFNGR endocytosis through clathrin-coated pits are independent events.

As well as in immune receptor signaling (Dykstra *et al.*, 2003), lipid rafts may also play a role in endocytosis (Johannes and Lamaze, 2002; Le Roy and Wrana, 2005; Rajendran and Simons, 2005). The IL-2 receptor is the first example of a cytokine receptor that is associated with DRMs and internalized through a clathrin-independent process (Lamaze *et al.*, 2001). The TGFβ receptor is another transmembrane receptor that is internalized through two distinct routes: clathrin-dependent endocytosis and a caveolar raft-associated pathway, each route being involved in distinct signaling events (Di Guglielmo *et al.*, 2003). The association of IFNGR with DRMs has led to the suggestion that lipid microdomains are selective sites of endocytosis of activated IFNGR complexes (Subramaniam and Johnson, 2002). Therefore, we tested whether, as well as a clathrin-dependent uptake, a subpopulation of IFNGR complexes was also internalized by a clathrin-independent uptake. Caveolae are unlikely to play a role in IFNGR uptake because we observed DRM association of activated IFNGR in Jurkat cells having no caveolae (unpublished data). Also, the inactivation of dynamin, which mediates both clathrin-dependent and caveolae/raft-dependent endocytosis (McNiven *et al.*, 2000), did not affect IFN-γ–induced signaling, further suggesting that IFN-γ signaling does not occur through clathrin-independent endocytosis. Finally, we were able to detect internalized IFNGR complexes associated with intracellular DRMs after endocytosis from the plasma membrane in control cells, but not when clathrin-dependent endocytosis was blocked (unpublished data). This showed that DRM association of activated IFNGR complexes occurred before they underwent endocytosis through clathrin-coated pits. We also considered that IFNGR complexes are regulated as recently described for the B-cell receptor. In this particular case, activated receptor uptake occurred only when clathrin was associated with DRMs and tyrosine phosphorylated through a Src-family kinase (Stoddart *et al.*, 2002). We found no specific tyrosine phosphorylation of the clathrin heavy chain by IFN-γ, nor did the selective Src family tyrosine kinase inhibitor PP2 inhibit IFNGR complex uptake (unpublished data). Altogether, these data demonstrate that the association of activated IFNGR complexes with lipid microdomains is required for initiating and propagating IFN-γ–induced signaling at the plasma membrane, but not for receptor uptake, which occurs through classical clathrin-dependent endocytosis. This explains why, unlike for IFN-α, IFN-γ signaling and biological activity were not affected by the inhibition of receptor endocytosis.

The alteration of the IFN-α–dependent long-term cellular response was unexpected as inhibition of Stat activation was transient and returned to control levels after 30 min. Whether the recovery of Stat was due to slow bulk membrane endocytosis or to an alternative signaling mechanism will need further investigation. In agreement with published data, our study shows that Stat activation by IFNs is maximal at 20–30 min and decreases quickly thereafter. Several genes can be activated by IFNs at times below 15 min (reviewed in Bach *et al.*, 1997; Stark *et al.*, 1998), and it has been shown that the response to IFN-α is controlled by the duration of stimulated Jak kinases activity (Lee *et al.*, 1997). Also, a Stat1 mutant that supports 20–30% normal transcription did not cause growth restraint (Bromberg *et al.*, 1996). When IFNAR endocytosis is blocked, it takes at least 30 min to restore normal levels of Jak kinases activity and Stat1 phosphorylation. As a result, activated Stat1 is present in insufficient amounts in the nucleus, and IFN-α–dependent transcriptional activity is inhibited by 50% 8 h after IFN-α stimulation. It is therefore likely that inhibition of IFNAR endocytosis prevents the transcription of early activated genes, some of which may be important to initiate full antiviral and antiproliferative activities. It will be important to test this hypothesis by correlating the kinetics of IFNAR endocytosis inhibition with the kinetics of transcription of early response genes that are specifically involved in the antiviral and antiproliferative response to IFN-α. Initial events in IFNAR trafficking and Stat1 activation are therefore critical to the onset of the Jak/Stat signaling cascade that leads to gene transcription, because even a transient perturbation of these early events can durably impair the biological responses to IFN-α.

Although the role of lipid microdomains in IFN-γ–dependent biological responses cannot be directly investigated in vivo, mice fed with omega-3 polyunsaturated fatty acids, a diet known to alter the stability and the composition of lipid microdomains in cell membranes, had defects in IFN-γ–induced Stat1 signaling and an impaired host resistance to *Listeria monocytogenes* (Irons and Fritsche, 2005). Recently, it has been shown that clathrin and raft-like microdomains may cooperate to internalize some signaling receptors such as the BCR or the EGF-R (Puri *et al.*, 2005; Stoddart *et al.*, 2005). This shows the increasing variety and complexity of the sorting events that originate at the plasma membrane and that there is no longer a clear distinction between clathrin-dependent and -independent endocytosis (Johannes and Lamaze, 2002). These studies highlight the need to understand better the contributions of these processes to the activation and trafficking of signaling receptors. The plasticity in the different endocytic pathways operating at the plasma membrane may limit the amount of new information that can be gained using classical quantitative endocytosis assays. Therefore, endocytosis studies will have to look at the various signaling receptors whose signal transduction is less flexible to reveal new regulations and to assess the functional role of a given endocytic pathway.

Our study has provided new insights into the interplay between plasma membrane compartmentalization, endocytosis, and signaling for IFN-α and IFN-γ receptor complexes. The differential regulation of Stat1, a common downstream effector of IFN-α and IFN-γ, through receptor clathrin-dependent endocytosis and lipid-based compartmentalization at the plasma membrane reveals the contribution of receptor sorting and trafficking to the signaling specificity of cytokines and the regulation of their biological activity within the Jak/Stat pathway.

ACKNOWLEDGMENTS

We thank the following people for kindly providing cells and reagents: A. Jackson, I. Bernard-Pierrot, Y. Gaudin, M. McNiven, S. Pellegrini, P. Stäheli, D. Stolz, A. Vidy, and J. Wietzerbin. We acknowledge the technical help from A. Saint-Pol, T. Falguières, and D. Pina. We thank S. Pelligrini and J. Wietzerbin for helpful discussions. This work was supported by grants from Ligue Nationale contre le Cancer, Association pour la Recherche sur le Cancer (5177), Fondation de France, and Action Concertée Incitative-Jeunes Chercheurs (5233). M.M. was supported by a fellowship from the Association pour la Recherche sur le Cancer and from the Curie Institute. M-N.M. was supported by fellowships from Association pour la Recherche sur le Cancer and Ligue Nationale contre le Cancer.

REFERENCES

Bach, E. A., Aguet, M., and Schreiber, R. D. (1997). The IFN gamma receptor: a paradigm for cytokine receptor signaling. Annu. Rev. Immunol. *15*, 563–591.

Benmerah, A., Lamaze, C., Bègue, B., Schmid, S. L., Dautry-Varsat, A., and Cerf-Bensussan, N. (1998). AP-2/Eps15 interaction is required for receptor-mediated endocytosis. J. Cell Biol. *140*, 1055–1062.

Bild, A. H., Turkson, J., and Jove, R. (2002). Cytoplasmic transport of Stat3 by receptor-mediated endocytosis. EMBO J. *21*, 3255–3263.

Brodsky, F. M., Chen, C. Y., Knuehl, C., Towler, M. C., and Wakeham, D. E. (2001). Biological basket weaving: formation and function of clathrin-coated vesicles. Annu. Rev. Cell. Dev. Biol. *17*, 517–568.

Bromberg, J. F., Horvath, C. M., Wen, Z., Schreiber, R. D., and Darnell, J. E., Jr. (1996). Transcriptionally active Stat1 is required for the antiproliferative effects of both interferon alpha and interferon gamma. Proc. Natl. Acad. Sci. USA *93*, 7673–7678.

Brown, D. A., and London, E. (2000). Structure and function of sphingolipid- and cholesterol-rich membrane rafts. J. Biol. Chem. *275*, 17221–17224.

Cajean-Feroldi, C., Nosal, F., Nardeux, P. C., Gallet, X., Guymarho, J., Baychelier, F., Sempe, P., Tovey, M. G., Escary, J. L., and Eid, P. (2004). Identification of residues of the IFNAR1 chain of the type I human interferon receptor critical for ligand binding and biological activity. Biochemistry *43*, 12498–12512.

Ceresa, B. P., and Schmid, S. L. (2000). Regulation of signal transduction by endocytosis. Curr. Opin. Cell Biol. *12*, 204–210.

Conner, S. D., and Schmid, S. L. (2003). Regulated portals of entry into the cell. Nature *422*, 37–44.

Damke, H., Baba, T., Warnock, D. E., and Schmid, S. L. (1994). Induction of mutant dynamin specifically blocks endocytic coated vesicle formation. J. Cell Biol. *127*, 915–934.

Di Fiore, P. P., and De Camilli, P. (2001). Endocytosis and signaling. an inseparable partnership. Cell *106*, 1–4.

Di Guglielmo, G. M., Le Roy, C., Goodfellow, A. F., and Wrana, J. L. (2003). Distinct endocytic pathways regulate TGF-beta receptor signalling and turnover. Nat. Cell Biol. *5*, 410–421.

Dykstra, M., Cherukuri, A., Sohn, H. W., Tzeng, S. J., and Pierce, S. K. (2003). Location is everything: lipid rafts and immune cell signaling. Annu. Rev. Immunol. *21*, 457–481. Epub 2001 Dec 2019.

Dykstra, M. L., Cherukuri, A., and Pierce, S. K. (2001). Floating the raft hypothesis for immune receptors: access to rafts controls receptor signaling and trafficking. Traffic *2*, 160–166.

Farrar, M. A., Campbell, J. D., and Schreiber, R. D. (1992). Identification of a functionally important sequence in the C terminus of the interferon-gamma receptor. Proc Natl Acad Sci USA *89*, 11706–11710.

Farrar, M. A., Fernandez-Luna, J., and Schreiber, R. D. (1991). Identification of two regions within the cytoplasmic domain of the human interferon-gamma receptor required for function. J. Biol. Chem. *266*, 19626–19635.

Filgueira, L., Groscurth, P., and Aguet, M. (1989). Binding and internalization of gold-labeled IFN-gamma by human Raji cells. J. Immunol. *142*, 3436–3439.

Fujimoto, M., and Naka, T. (2003). Regulation of cytokine signaling by SOCS family molecules. Trends Immunol. *24*, 659–666.

Harder, T., and Engelhardt, K. R. (2004). Membrane domains in lymphocytes—from lipid rafts to protein scaffolds. Traffic *5*, 265–275.

Irons, R., and Fritsche, K. L. (2005). Omega-3 polyunsaturated fatty acids impair in vivo interferon-gamma responsiveness via diminished receptor signaling. J. Infect. Dis. *191*, 481–486. Epub 2004 Dec 2028.

Johannes, L., and Lamaze, C. (2002). Clathrin-dependent or not: is it still the question? Traffic *3*, 443–451.

Kerr, I. M., Costa-Pereira, A. P., Lillemeier, B. F., and Strobl, B. (2003). Of JAKs, STATs, blind watchmakers, jeeps and trains. FEBS Lett. *546*, 1–5.

Kisseleva, T., Bhattacharya, S., Braunstein, J., and Schindler, C. W. (2002). Signaling through the JAK/STAT pathway, recent advances and future challenges. Gene *285*, 1–24.

Lamaze, C., Dujeancourt, A., Baba, T., Lo, C. G., Benmerah, A., and Dautry-Varsat, A. (2001). Interleukin 2 receptors and detergent-resistant membrane domains define a clathrin-independent endocytic pathway. Mol. Cell *7*, 661–671.

Lee, C. K., Bluyssen, H. A., and Levy, D. E. (1997). Regulation of interferon-alpha responsiveness by the duration of Janus kinase activity. J. Biol. Chem. *272*, 21872–21877.

Le Roy, C., and Wrana, J. L. (2005). Clathrin- and non-clathrin-mediated endocytic regulation of cell signalling. Nat. Rev. Mol. Cell. Biol. *6*, 112–126.

Levy, D. E., and Darnell, J. E., Jr. (2002). Stats: transcriptional control and biological impact. Nat. Rev. Mol. Cell. Biol. *3*, 651–662.

Li, X., Leung, S., Kerr, I. M., and Stark, G. R. (1997). Functional subdomains of STAT2 required for preassociation with the alpha interferon receptor and for signaling. Mol. Cell. Biol. *17*, 2048–2056.

McNiven, M. A., Cao, H., Pitts, K. R., and Yoon, Y. (2000). The dynamin family of mechanoenzymes: pinching in new places. Trends Biochem. Sci. *25*, 115–120.

Miaczynska, M., Pelkmans, L., and Zerial, M. (2004). Not just a sink: endosomes in control of signal transduction. Curr. Opin. Cell Biol. *16*, 400–406.

Mogensen, K. E., Lewerenz, M., Reboul, J., Lutfalla, G., and Uze, G. (1999). The type I interferon receptor: structure, function, and evolution of a family business. J. Interferon Cytokine Res. *19*, 1069–1098.

Munro, S. (2003). Lipid rafts: elusive or illusive? Cell *115*, 377–388.

O'Shea, J. J., Gadina, M., and Schreiber, R. D. (2002). Cytokine signaling in 2002, new surprises in the Jak/Stat pathway. Cell *109*, S121–S131.

Parton, R. G., and Richards, A. A. (2003). Lipid rafts and caveolae as portals for endocytosis: new insights and common mechanisms. Traffic *4*, 724–738.

Puri, C., Tosoni, D., Comai, R., Rabellino, A., Segat, D., Caneva, F., Luzzi, P., Di Fiore, P. P., and Tacchetti, C. (2005). Relationships between EGFR signaling-competent and endocytosis-competent membrane microdomains. Mol. Biol. Cell *16*, 2704–2718. Epub 2005 Mar 2716.

Rajendran, L., and Simons, K. (2005). Lipid rafts and membrane dynamics. J. Cell Sci. *118*, 1099–1102.

Rubinstein, S., Familletti, P. C., and Pestka, S. (1981). Convenient assay for interferons. J. Virol. *37*, 755–758.

Saint-Pol, A. *et al.* (2004). Clathrin adaptor epsinR is required for retrograde sorting on early endosomal membranes. Dev. Cell *6*, 525–538.

Schindler, C., and Brutsaert, S. (1999). Interferons as a paradigm for cytokine signal transduction. Cell Mol. Life Sci. *55*, 1509–1522.

Schroder, K., Hertzog, P. J., Ravasi, T., and Hume, D. A. (2003). Interferon-{gamma}: an overview of signals, mechanisms, and functions. J. Leukoc. Biol. *2*, 2.

Sharma, P., Varma, R., Sarasij, R. C., Ira, Gousset, K., Krishnamoorthy, G., Rao, M., and Mayor, S. (2004). Nanoscale organization of multiple GPI-anchored proteins in living cell membranes. Cell *116*, 577–589.

Shenoy, S. K., and Lefkowitz, R. J. (2003). Multifaceted roles of beta-arrestins in the regulation of seven-membrane-spanning receptor trafficking and signalling. Biochem. J. *375*, 503–515.

Shuai, K., and Liu, B. (2003). Regulation of JAK-STAT signalling in the immune system. Nat. Rev. Immunol. *3*, 900–911.

Silver, D. L., Geisbrecht, E. R., and Montell, D. J. (2005). Requirement for JAK/STAT signaling throughout border cell migration in *Drosophila.* Development *132*, 3483–3492. Epub 2005 Jul 3486.

Simons, K., and Ikonen, E. (1997). Functional rafts in cell membranes. Nature *387*, 569–572.

Sorkin, A., and Von Zastrow, M. (2002). Signal transduction and endocytosis: close encounters of many kinds. Nat. Rev. Mol. Cell. Biol. *3*, 600–614.

Stark, G., Kerr, I., Williams, B., Silverman, R., and Schreiber, R. (1998). How cells respond to interferons. Annu. Rev. Biochem. *67*, 227–264.

Stoddart, A., Dykstra, M. L., Brown, B. K., Song, W., Pierce, S. K., and Brodsky, F. M. (2002). Lipid rafts unite signaling cascades with clathrin to regulate BCR internalization. Immunity *17*, 451–462.

Stoddart, A., Jackson, A. P., and Brodsky, F. M. (2005). Plasticity of B cell receptor internalization upon conditional depletion of clathrin. Mol. Biol. Cell *16*, 2339–2348.

Stolz, D. B., Ross, M. A., Salem, H. M., Mars, W. M., Michalopoulos, G. K., and Enomoto, K. (1999). Cationic colloidal silica membrane perturbation as a means of examining changes at the sinusoidal surface during liver regeneration. Am. J. Pathol. *155*, 1487–1498.

Subramaniam, P. S., and Johnson, H. M. (2002). Lipid microdomains are required sites for the selective endocytosis and nuclear translocation of IFN-gamma, its receptor chain IFN-gamma receptor-1, and the phosphorylation and nuclear translocation of STAT1alpha. J. Immunol. *169*, 1959–1969.

Takaoka, A., Mitani, Y., Suemori, H., Sato, M., Yokochi, T., Noguchi, S., Tanaka, N., and Tanaguchi, T. (2000). Cross talk between interferon-gamma and -alpha/beta signaling components in caveolar membrane domains. Science *288*, 2357–2360.

Taniguchi, T., and Takaoka, A. (2001). A weak signal for strong responses: interferon-alpha/beta revisited. Nat. Rev. Mol. Cell. Biol. *2*, 378–386.

Tiwari, R. K., Kusari, J., and Sen, G. C. (1987). Functional equivalents of interferon-mediated signals needed for induction of an mRNA can be generated by double-stranded RNA and growth factors. EMBO J. *6*, 3373–3378.

Vieira, A. V., Lamaze, C., and Schmid, S. L. (1996). Control of EGF receptor signaling by clathrin-mediated endocytosis. Science *274*, 2086–2089.

Wiley, S., and Burke, P. (2001). Regulation of receptor tyrosine kinases signaling by endocytic trafficking. Traffic *2*, 12–18.

Zoon, K. C., Arnheiter, H., Zur Nedden, D., Fitzgerald, D. J., and Willingham, M. C. (1983). Human interferon alpha enters cells by receptor-mediated endocytosis. Virology *130*, 195–203.